

Green Synthesis of Gold Nanoparticles using American Ginseng and Their Characterization

Article History

Received: 15-Jun-2025

Revised: 28-Jul-2025

Accepted: 30-Jul-2025

Published: 13-Aug-2025

Emma Klatt^{a#}, Benjamin Lilienkamp^{a#}, Sonia Grade^a, Paige Bowman^a, Yale Wang^b, Anna DeBruine^a, Keagan Schmidt^a, Matey Kaltchev^a, Junhong Chen^{c,d}, Aakash Gupta^e, Qingsu Cheng^e, Wujie Zhang^{a*}

Abstract: Gold nanoparticles have a wide variety of applications in biomedical fields such as biosensing, cancer treatment, drug delivery, and bioimaging. This research focuses on using American ginseng (*Panax quinquefolium*), specifically the leaves, as a plant-mediated green synthesis process to produce gold nanoparticles (Au NPs). Various extracts (leaf, stem, and root) were compared for Au NP synthesis. The leaf extract was found to be the most effective; hence, they were used for Au NPs synthesis. Plant extract Au NPs were characterized using UV-vis spectroscopy, scanning electron microscopy-energy-dispersive X-ray spectroscopy (SEM-EDX), atomic force microscopy (AFM), attenuated total reflection Fourier transform infrared spectroscopy (ATR-FTIR), dynamic light scattering (DLS), and X-ray diffraction (XRD). The results showed that the leaves could produce spherical Au NPs that were well dispersed with an average diameter of around 18 nm. The nanoparticles also had a characteristic absorbance peak at ~529 nm. A cytotoxicity study was conducted using HeLa cells, and the cell number decreased as the concentration of the Au NPs increased, although the cell viability remained high (>99 %). Au NPs produced using the American ginseng leaves show great potential for various applications, such as drug delivery, imaging and diagnostics, and therapy.

Keywords: American ginseng; Green Synthesis; Nanoparticle; Cytotoxicity; Bioinspired

a Chemical and Biomolecular Engineering Program, Physics and Chemistry Department, Milwaukee School of Engineering, Milwaukee, WI 53202, USA

b Mechanical Engineering Department, University of Wisconsin-Milwaukee, Milwaukee, WI 53211, USA

c Pritzker School of Molecular Engineering, University of Chicago, Chicago, IL 60637, USA

d Chemical Sciences and Engineering Division and Center for Molecular Engineering, Argonne National Laboratory, Lemont, IL 60439, USA

e Biomedical Engineering Department, University of Wisconsin-Milwaukee, Milwaukee, WI 53211, USA

Equal contribution

* **Corresponding author:** Email: zhang@msoe.edu

1. INTRODUCTION

Nanoparticles are particles ranging from 1 to 100 nanometers in size and have gained traction due to their application in areas such as biomedical, environmental, microelectronics, catalysis, and food packaging (Chen *et al.*, 2025; Ghobashy *et al.*, 2024; Kumar *et al.*, 2021; Shahalaei *et al.*, 2024; Vijayaram *et al.*, 2024). Particularly in biomedical applications, Au NPs exhibit surface properties that can be utilized via attachments of various components (drugs, radioisotopes, fluorescent dyes, *etc.*) for drug and gene delivery, bioimaging and diagnostics, as well as photothermal and photodynamic therapies (Anik *et al.*, 2022; Ghobashy *et al.*, 2024; Kumari *et al.*, 2023; Milan *et al.*, 2022; Nejati *et al.*, 2022).

Chemical and physicochemical methods are traditionally utilized for producing gold nanoparticles (Au NPs); however, these methods lead to concerns such as negative environmental impacts and high energy consumption, which may potentially restrict their applications. In contrast, biological and green synthesis approaches apply intrinsic biomolecules from the bio machinery or plant extract, enabling multifaceted,

© The Author(s), 2025

biocompatible nanomaterials production through an environmentally sustainable and economical route. Regarding green synthesis, organisms like plants, bacteria, algae, and fungi have been found to contain phytochemicals essential for green synthesis and the stabilization of nanoparticles. Examples of plant extracts utilized for green synthesis of Au NPs are *Litsea cubeba* (May Chang), *Barbarea verna* (upland cress), *Brazilian red propolis* (honeybee product), *Chlorella vulgaris* (algae), *Halodule uninervis* (seagrass), *Mimosa tenuiflora* (Jurema) and *Ziziphus ziziphus* (Jujube) (Aljabali et al., 2018; Annamalai & Nallamuthu, 2015; Botteon et al., 2021; Doan et al., 2020; Hutchinson et al., 2022; Rodríguez-León et al., 2019; Wehbe et al., 2025).

American ginseng (*panax quinquefolium*), which is found in regions of North America and over 95% of which is produced in Wisconsin, exhibits antimicrobial and anti-diabetic effects as it increases insulin sensitivity (Szczuka et al., 2019; Werner et al., 2014). American ginseng has also been reported to alleviate cancer-related fatigue (Lemke, 2021). Generally, the roots are harvested and purified for tea, while the leaves are discarded, so there is a desire to find use for the otherwise wasted leaves (Kang & Kim, 2016). The objective of this study was to investigate the possibility of using American ginseng leaves for the synthesis of metallic nanoparticles and their subsequent characterization for potential biomedical applications, particularly in cancer treatment. Plant-based Au NPs offer advantages over chemically synthesized counterparts due to their biocompatibility and pronounced anticancer therapeutic and diagnostic efficacy (Bharadwaj et al., 2021). For instance, a recent study demonstrated that Au NPs synthesized using *Halodule uninervis* ethanolic extract inhibited the proliferation of several cancer cell lines *in vitro* (Wehbe et al., 2025).

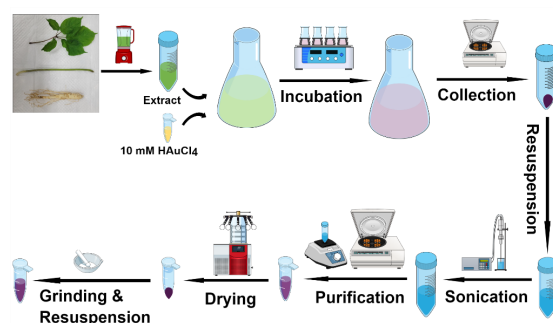
2. MATERIALS AND METHODS

2.1. Materials

American ginseng (Marathon Ginseng, Marathon County, Wisconsin) was authenticated and purchased directly from Marathon ginseng and stored at 4°C. Gold (III) chloride trihydrate (HAuCl₄; 520918), 4-nitrophenol (C₆H₅NO₃; 241326), Folin-Ciocalteu reagent (F9252), gallic acid (G7384), and sodium borohydride (NaBH₄; 80637300) were obtained from MilliporeSigma (St. Louis, MO, USA) and were used as received.

2.2. Green Synthesis of Au NPs

The green synthesis and purification process (Scheme 1) followed previous work (Hutchinson et al., 2022; Johnson et al., 2020). Briefly, 10 g of American ginseng leaf, stem, or root were blended with 100 mL of deionized (DI) water for 15 s to produce the respective extracts. The extracts were then vacuum filtered twice (Whatman filter paper) and centrifuged at 4,000 rpm for 5 min to yield the supernatant. Finally, 5 mL of each type of extract, 10 mM gold (III) chloride trihydrate (0.4 mL), and DI water (35 mL) were mixed in a flask, then placed in an incubator shaker at 215 rpm and 37°C for 6 h.



Scheme 1. Green synthesis process of Au NPs using American ginseng: from extract preparation to nanoparticle purification.

After synthesis, Au NPs were purified according to (Hutchinson et al., 2022; Johnson et al., 2020). The nanoparticles were first collected using centrifugation at 4,000 rpm for 20 min. The particles were then suspended in 10 mL of DI water and sonicated for 5 min. The mixture was centrifuged again at 4,000 rpm for 20 min. The obtained nanoparticles were subjected to a series of wash/vortex and centrifugation cycles with Triton X-114 (0.75 µL/mL DI water), acetone, isopropyl alcohol, and DI water, respectively. After these washes, the nanoparticles were then freeze-dried and stored in the freezer at -20°C for further characterization.

2.3. Characterization of Au NPs

UV-visible spectroscopy (Evolution 60S; Thermo Fisher Scientific, Waltham, MA) was performed to analyze the Au NPs during the synthesis process. The mixtures were scanned from 350 to 650 nm wavelengths every hour. Scanning electron microscopy (FE-SEM, Hitachi S-4800 ultra-high resolution cold cathode field emission scanning electron

microscope, Kefeld, Germany) coupled with energy dispersive X-ray spectroscopy (EDX, Noran (Si(Li)) detector, Thermo Fisher Scientific, Waltham, MA, USA) was used to image and determine the elemental composition of the Au NPs. SEM images were analyzed by NIH ImageJ software for size measurements. Freeze-dried Au NPs were also analyzed using attenuated total reflection Fourier transform infrared (ATR-FTIR; MIRacle 10, IR-Tracer 100; Shimadzu, Kyoto, Japan) spectroscopy. Atomic force microscopy (AFM) images, using an Au NP solution, were taken using contact mode on a Bruker MultiMode atomic force microscope with a Nanoscope 6 controller (Santa Barbara, CA, USA). The hydrodynamic diameter and zeta (ζ) potential of the Au NPs were determined using a dynamic light scattering (DLS) instrument (DLS; Litesizer DLS 700, Anton Paar, Austria). Powder X-ray diffraction (XRD) analysis was conducted using a Bruker D8 Discover X-ray diffractometer (Billerica, MA, USA) to confirm the crystalline structure of the Au NPs.

2.4. Cytotoxicity Study

HeLa cells (purchased from ATCC) were cultured in Eagles Minimum Essential Medium (EMEM). The medium was supplemented with 10% fetal bovine serum, 100 U mL⁻¹ penicillin, and 100 mg/L streptomycin. After being cultured in a humidified CO₂ incubator (5%) at 37°C, cells were seeded at a density of 5×10^4 cells/well into a 24-well plate. After 24-hour incubation, the medium was replaced with fresh medium containing various Au NP concentrations in quadruplicate (0, 0.1, 0.5, 1.0, 1.75, and 2.5 mM).

After a 24-hour incubation period, cells were rinsed twice with Dulbecco's Phosphate-Buffered Saline (DPBS). 455 μ L Hoechst-33342 (62249; Thermo Fisher Scientific, Waltham, MA, USA) and

455 μ L calcein-AM/ethidium homodimer-1 (LIVE/DEAD™ Viability/Cytotoxicity Kit, for mammalian cells; Thermo Fisher Scientific, Waltham, MA, USA) were added to each well for staining nuclei and live/dead cells (final concentration of 5 μ M each), respectively. After incubating for 5-min, cells were examined under an EVOS fluorescent microscope (Thermo Fisher Scientific, Waltham, MA, USA), and images were taken at different locations per well. Cell number and viability were determined using the ImageJ software. Cell viabilities were determined using the following equation:

$$\frac{\text{Number of live cells}}{\text{Total number of cells}} \times 100\%.$$

3. RESULTS AND DISCUSSION

3.1. Total Phenolic and Ascorbic Acid Contents of Different Extracts

The total phenolic and ascorbic acid contents are critical indicators for metallic nanoparticle green synthesis. The plant extracts were blended to obtain the necessary phytochemicals (e.g., phenolics and ascorbic acid) within American ginseng to serve as a reducing agent for reducing gold (III) chloride trihydrate and a capping agent. Generally, the higher the contents are, the more effective the extract can be as a reducing agent (Zhang *et al.*, 2015). To determine which extract of American ginseng had the highest reducing capability, the contents of each extract were determined. As expected, the total phenolic and ascorbic acid contents were both highest for the leaf extract, 352.75 \pm 60.07 μ g GAE/mL and 75.54 \pm 8.98 μ g/mL, respectively (Fig. 1 and Table 1). It is also worth noting that the leaf extract was the easiest to prepare, particularly in terms of filtration to remove plant material (Table 1).

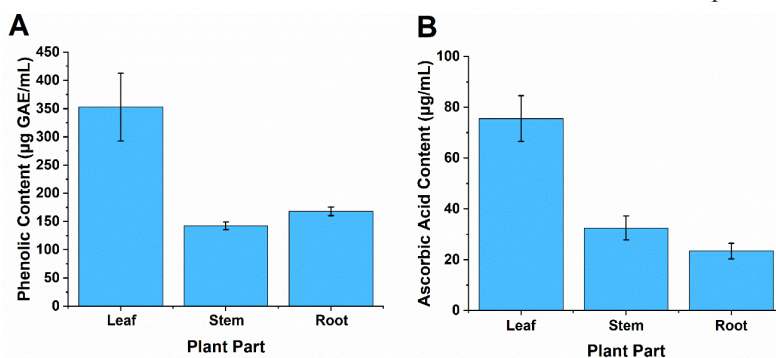


Figure 1. The phenolic compound and ascorbic acid contents of the leaf, stem, and root extracts.

Table 1. Comparison of various American ginseng extracts and their effects on Au NP synthesis.

| Extract | Extract Preparation | Reducing/Capping Agents | | Absorbance (λ_{max}) | |
|---------|---------------------|---|------------------------------------|---------------------------------------|------------------|
| | | Phenolic Compounds ($\mu\text{g GAE/mL}$) | Ascorbic Acid ($\mu\text{g/mL}$) | 1 hr | 6 hr |
| Leaf | Easy | 352.75 ± 60.07 | 75.54 ± 8.98 | 0.12777 (532 nm) | 0.21054 (538 nm) |
| Stem | Difficult | 142.50 ± 6.82 | 32.53 ± 4.76 | 0.04917 (538 nm) | 0.13042 (554 nm) |
| Root | Difficult | 168.10 ± 7.75 | 23.43 ± 3.10 | 0.04439 (534 nm) | 0.07425 (550 nm) |

3.2. Effects of Incubation Time on Green Synthesis Process

Au NPs have optical properties that indicate the successful synthesis of nanoparticles. The transition from a dilute green to a reddish-purple color (Fig. 2) indicates the formation of Au NPs. This transition is due to the plasmon resonance phenomenon when a light photon hits a metal surface, most often gold (Hutchinson *et al.*, 2022). Localized surface plasmon resonance occurs when the frequency of incident photons resonates with the collective oscillation of conduction electrons in metal nanoparticles. Plasmonic nanoparticles can absorb light in the visible region, and their peak absorbance wavelength strongly depends on the shape and size of the nanoparticles (Kaur *et al.*, 2021; Semwal *et al.*, 2023). As the green synthesis progresses, the color deepens and the absorbance intensity increases. Both color and absorbance intensity changes indicate that the leaf extract is the most effective at synthesizing Au NPs. For leaf extract the purple color is visible even within 1 h, while the other extracts do not show visible color change until 2–3 h. This indicates that nucleation began more rapidly in the mixture containing the leaf extract, likely due to its relatively high content of reducing agents. The green synthesis was monitored at different periods by recording the spectrum of each mixture. As shown in the UV-visible spectra of Fig. 3 and Table 1, the right shift of the peak (550 nm) and intensity increase between 1- and 3-h samples for each particle indicated the growth of Au NPs and/or an increased number of particles. The intensity difference between 3- and 6-h samples was insignificant for the leaf or root. There was a difference in intensity between the 3- and 6-h stem samples, but the leaf consistently exhibited the highest absorbance intensity, indicating it is the most optimal extract for Au NP synthesis. This is largely attributed to the rapid nucleation and greater num-

ber of nuclei (or seeds) formed during the synthesis process in the presence of the leaf extract. Hence, leaf extract was selected for Au NP synthesis and further studies.

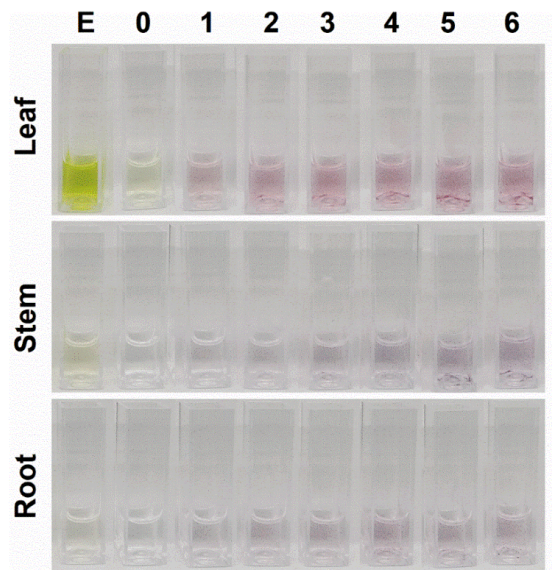


Figure 2. Color change of the different American ginseng extract and gold (III) chloride trihydrate mixtures over a 6-hour period with 1-hour intervals. The observed color change serves as a visual indicator of Au NP formation.

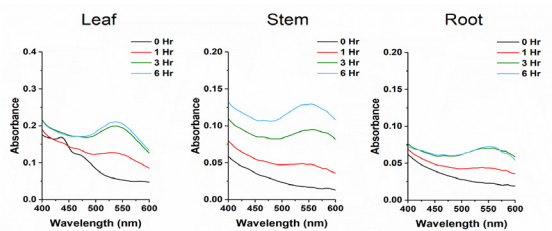


Figure 3. UV-vis spectra of the different plant extracts and gold (III) chloride trihydrate mixtures at different incubation times, monitoring the formation and growth of Au NPs.

3.3. Morphology, Crystal Structure, and Chemical Composition

Due to their intense resolution capabilities, SEM and AFM provide high-definition visualization of gold nanoparticles. An SEM image of Au NPs is shown in **Fig. 4A**. Au NPs can be seen as small bright spots in the image, and they are uniformly distributed spherical particles, confirming the successful green synthesis process. The diameter of the Au NPs was determined to be 17.9 ± 2.2 nm using the SEM image and NIH ImageJ. An AFM image (**Fig. 4B**) also exhibits the well-dispersed spherical shape of the Au NPs. **Fig. 4C** depicts the EDX spectrum showing the characteristic peaks of gold element, which verifies the chemical composition of the gold in the nanoparticles with a 40.63% gold composition by mass (8.88% by atom). The Au NPs that were synthesized by American ginseng had a higher gold content than those synthesized by upland cress (11.13%) (Hutchinson *et al.*, 2022).

Carbon (23.99% by mass) and oxygen (1.92% by mass) peaks within the EDX spectrum also indicate the presence of bioactive phytochemicals (Liu *et al.*, 2020; Szczuka *et al.*, 2019). As shown in **Fig. 4D**, the hydrodynamic diameter of the Au NPs was determined to be 9.6 ± 3.1 nm. The size differences observed across characterization techniques can be attributed to the sample state and the underlying measurement principles of each method. The average ζ -potential was -29.2 mV, indicating good nanoparticle stability (Fouda *et al.*, 2022; Hutchinson *et al.*, 2022). XRD analysis (**Fig. 5**) revealed diffraction peaks at 2θ angles of 37.9° , 43.8° , 64.5° , 77.3° , and 81.6° , corresponding to the crystalline gold planes (111), (200), (220), (311), and (222), confirming the expected face-centered cubic structure (JCPDS Card No. 96-901-1613). The unassigned diffraction peaks are attributed to the formation of bio-organic crystallite phases on the surface of the Au NPs (Hutchinson *et al.*, 2022).

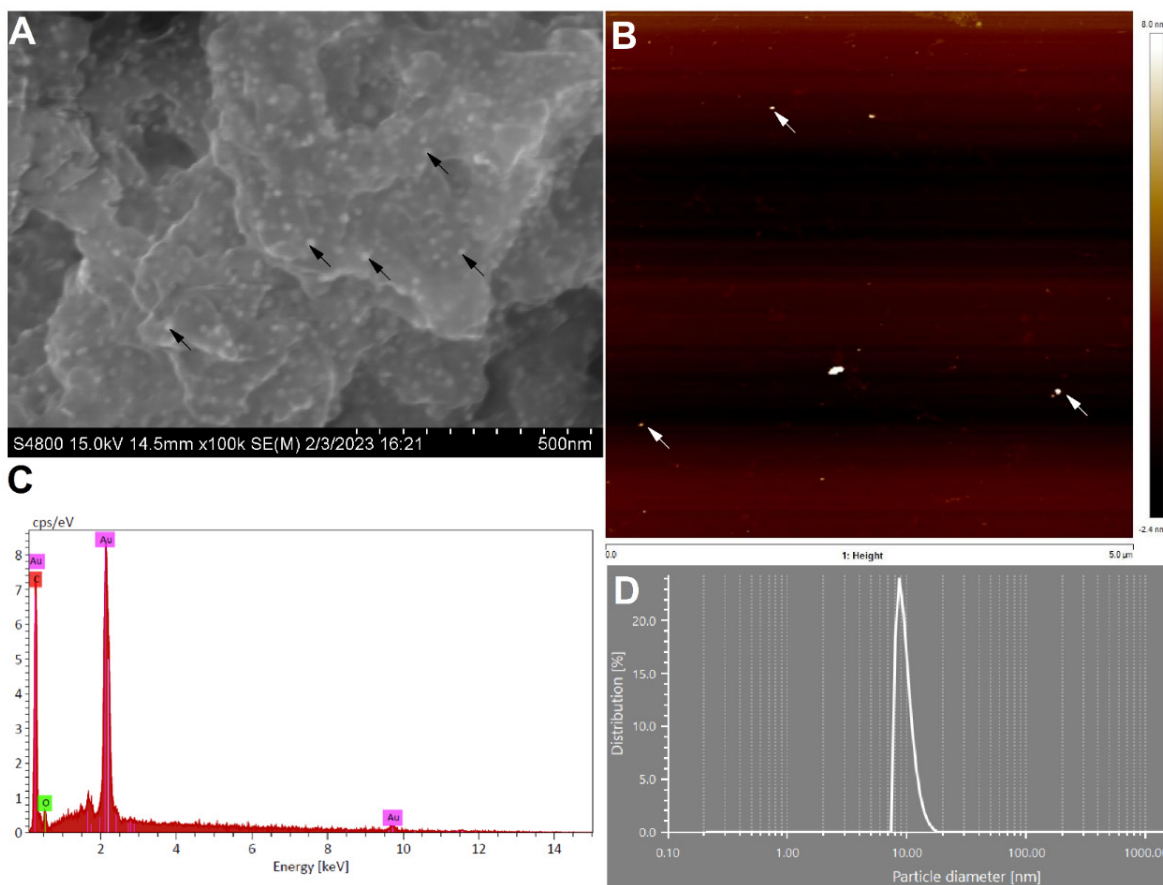


Figure 4. SEM image (A), AFM image (B), EDX spectrum (C), and DLS size distribution (D) of the synthesized Au NPs. Scale bar: 500 nm. The arrows point to some of the Au NPs (A & C).

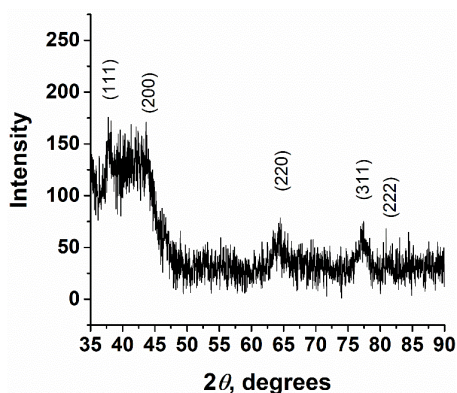


Figure 5. Powder XRD spectrum of the synthesized Au NPs.

The ATR-FTIR spectrum of Au NPs is shown in **Fig. 6**. Comparing the spectra of leaf extract and the Au NPs, although there is a strong resemblance, it can be concluded that not all the molecules were involved in stabilizing/capping Au NPs. The Au NP spectrum peaks can be correlated with their associated functional groups based on prior research (Hutchinson *et al.*, 2022; Pourhassan-Moghaddam *et al.*, 2014; Wehbe *et al.*, 2025). The peak assignments include 3289 cm^{-1} ($-\text{OH}$ and $-\text{NH}$ stretching of alcohols, phenolics and proteins), 2930 cm^{-1} and 2873 cm^{-1} ($-\text{CH}$ stretching of alkanes), 1648 cm^{-1} ($-\text{NH}$ bending, $-\text{C}=\text{C}$, $-\text{NO}$, $-\text{N}=\text{N}$, $-\text{C}=\text{N}$, and $-\text{C}=\text{O}$ stretching of proteins), 1515 cm^{-1} ($-\text{CH}$ alkane stretching, $-\text{NO}$ of nitro-compounds like glucosinolates), 1453 cm^{-1} ($-\text{OH}$ bending, $-\text{C}=\text{O}$ of phenolics, alcohols, and proteins), 1390 cm^{-1} ($-\text{CN}$ stretching of aromatic amine group), 644 cm^{-1} ($-\text{CH}$ bending of hydrocarbons). Overall, the peaks observed in the range of 1600 to 500 cm^{-1} are characteristic of polyphenols. According to these results, phenolics, alcohols, and other phytochemicals are present on the surface of the Au NPs.

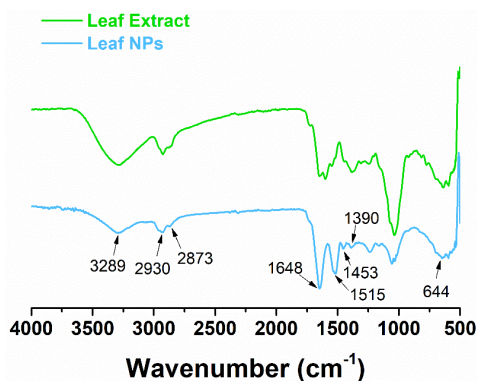


Figure 6. ATR-FTIR spectra of American ginseng leaf extract and the Au NPs synthesized using the leaf extract.

3.4. Cytotoxicity Analysis

Considering that Au NPs have been widely used in cancer treatment, such as drug delivery and imaging, HeLa cells (human cervical cancer cells) were used for investigating the green-synthesized Au NPs. As shown in **Fig. 7A**, there was an expected decrease in the number of cells after incubation compared to the control group with an increase in Au NP concentration. This can be explained as the increased cellular uptake of nanoparticles at a higher Au NP concentration. However, with the highest concentration (2.50 mM), the number of cells increased, which is most likely due to the aggregation of Au NPs at a high concentration, thereby reducing the cellular uptake. With no group having a viability less than 99% (**Fig. 7B**), it can be concluded that the presence of Au NPs did not lead to cell death, but rather inhibited the proliferation of HeLa cells. These results indicate that the Au NPs are less toxic to mammalian human cells than the Au NPs synthesized by upland crest (Hutchinson *et al.*, 2022). Au NPs in general interfere with the formation of cytoskeletal structures, which can inhibit DNA replication and cause DNA damage through oxidative stress. Oxidative stress, along with decreasing cell membrane integrity, ultimately hinders cell proliferation (Kus-Liśkiewicz *et al.*, 2021; Lee *et al.*, 2019). Other mechanisms include mitochondrial dysfunction and caspase activation (Bharadwaj *et al.*, 2021).

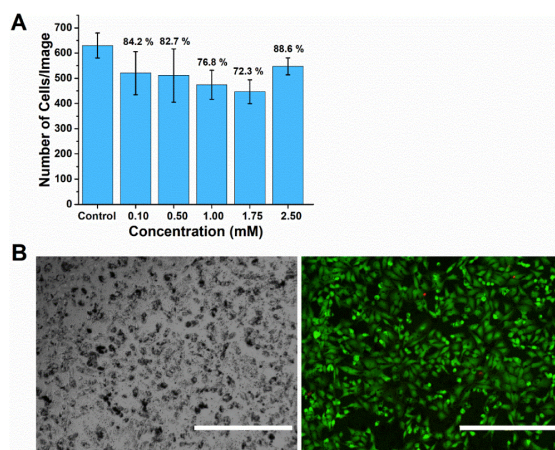


Figure 7. Average cell numbers after 24-hour incubation with the synthesized Au NPs at different concentrations (A). Percentages indicate the number of cells in each experimental group relative to the control group. A representative set of images of cells, bright field (left) and merged fluorescent (right), showing high cell viability after 24-hour incubation with synthesized Au NPs is presented in (B). Green: live cells, Red: dead/dying cells. Scale bar: 400 μm .

4. CONCLUSIONS

This work focused on the potential usage of American ginseng leaves as a green synthesis agent to produce Au NPs. UV-vis spectroscopy and gold (III) chloride trihydrate solution color change characterized the purified particles from the leaf, stem, and root. The results from the UV-vis spectroscopy and the visual color change confirmed that the leaf was the most effective in synthesizing Au NPs. As such, all the subsequent tests (SEM-EDX, AFM, ATR-FTIR, DLS, and XRD) were done with leaf extract synthesized Au NPs. The synthesized Au NPs had an even distribution and spherical shape. The cytotoxicity study indicated that the number of cells was Au NP concentration dependent. As the concentration of Au NPs moderately increased, the number of cells per image decreased, although the cell viability remained high with all the groups above 99%. Overall, utilizing American ginseng leaves to produce gold nanoparticles is eco-friendly, cost-effective, and efficient. The nanoparticles synthesized from the leaf extract demonstrate significant potential for a wide range of applications, particularly in cancer therapeutics. Future directions include investigating the inhibitory mechanisms of green-synthesized Au NPs on cancer cell proliferation, modifying these nanoparticles for gene and drug delivery, and exploring their applications in bioimaging, biosensing, as well as in photothermal and photodynamic therapies.

Data Availability Statement: The data that support the findings of this study are available from the corresponding author upon reasonable request.

Acknowledgements: The work was partially financially supported by the National Science Foundation (EEC—2045738). The authors would like to acknowledge Dr. Michael Navin and De'Jorra Valentin for their technical support.

Conflicts of Interest: The authors declare no conflict of interest.

References

- Aljabali, A. A. A., Akkam, Y., Al Zoubi, M. S., Al-Batayneh, K. M., Al-Trad, B., Abo Alrob, O., Alkilany, A. M., Benamara, M., & Evans, D. J. (2018). Synthesis of Gold Nanoparticles Using Leaf Extract of *Ziziphus zizyphus* and their Antimicrobial Activity. *Nanomaterials*, 8(3), 174. <https://www.mdpi.com/2079-4991/8/3/174>
- Anik, M. I., Mahmud, N., Al Masud, A., & Hasan, M. (2022). Gold nanoparticles (GNPs) in biomedical and clinical applications: A review. *Nano Select*, 3(4), 792–828. <https://doi.org/10.1002/nano.202100255>
- Annamalai, J., & Nallamuthu, T. (2015). Characterization of biosynthesized gold nanoparticles from aqueous extract of *Chlorella vulgaris* and their anti-pathogenic properties. *Applied Nanoscience*, 5(5), 603–607. <https://doi.org/10.1007/s13204-014-0353-y>
- Bharadwaj, K. K., Rabha, B., Pati, S., Sarkar, T., Choudhury, B. K., Barman, A., Bhattacharjya, D., Srivastava, A., Baishya, D., Edinur, H. A., Abdul Kari, Z., & Mohd Noor, N. H. (2021). Green Synthesis of Gold Nanoparticles Using Plant Extracts as Beneficial Prospect for Cancer Theranostics. *Molecules*, 26(21), 6389. <https://www.mdpi.com/1420-3049/26/21/6389>
- Botteon, C. E. A., Silva, L. B., Ccana-Ccapatinta, G. V., Silva, T. S., Ambrosio, S. R., Veneziani, R. C. S., Bastos, J. K., & Marcato, P. D. (2021). Biosynthesis and characterization of gold nanoparticles using Brazilian red propolis and evaluation of its antimicrobial and anticancer activities. *Scientific Reports*, 11(1), 1974. <https://doi.org/10.1038/s41598-021-81281-w>
- Chen, Y., Zohaib, A., Sun, H., & Sun, S. (2025). Multi-metallic nanoparticles: synthesis and their catalytic applications [10.1039/D5CC01468A]. *Chemical Communications*. <https://doi.org/10.1039/D5CC01468A>
- Doan, V.-D., Thieu, A. T., Nguyen, T.-D., Nguyen, V.-C., Cao, X.-T., Nguyen, T. L.-H., & Le, V. T. (2020). Biosynthesis of Gold Nanoparticles Using Litsea cubeba Fruit Extract for Catalytic Reduction of 4-Nitrophenol. *Journal of Nanomaterials*, 2020(1), 4548790. <https://doi.org/10.1155/2020/4548790>
- Fouda, A., Eid, A. M., Guibal, E., Hamza, M. F., Hassan, S. E.-D., Alkhalifah, D. H. M., & El-Hossary, D. (2022). Green Synthesis of Gold Nanoparticles by Aqueous Extract of *Zingiber officinale*: Characterization and Insight into Antimicrobial, Antioxidant, and In Vitro Cytotoxic Activities. *Applied Sciences*, 12(24), 12879. <https://www.mdpi.com/2076-3417/12/24/12879>
- Ghobashy, M. M., Alkhursani, S. A., Alqahtani, H. A., El-damhougy, T. K., & Madani, M. (2024). Gold nanoparticles in microelectronics advancements and biomedical applications. *Materials Science*

- and Engineering: B, 301, 117191. <https://doi.org/https://doi.org/10.1016/j.mseb.2024.117191>
- Hutchinson, N., Wu, Y., Wang, Y., Kanungo, M., DeBruine, A., Kroll, E., Gilmore, D. J., Eckrose, Z., Gaston, S., Matel, P., Kaltchev, M., Nickel, A.-M., Kumpaty, S., Hua, X., & Zhang, W. (2022). Green Synthesis of Gold Nanoparticles Using Upland Cress and Their Biochemical Characterization and Assessment. *Nanomaterials*, 12(1), 28. <https://www.mdpi.com/2079-4991/12/1/28>
- Johnson, D. L., Wang, Y., Stealey, S. T., Alexander, A. K., Kaltchev, M. G., Chen, J., & Zhang, W. (2020). Biosynthesis of silver nanoparticles using upland cress: purification, characterisation, and antimicrobial activity. *Micro & Nano Letters*, 15(2), 110–113. <https://doi.org/https://doi.org/10.1049/mnl.2019.0528>
- Kang, O. J., & Kim, J. S. (2016). Comparison of Ginsenoside Contents in Different Parts of Korean Ginseng (*Panax ginseng* C.A. Meyer). *Preventive Nutrition and Food Science*, 21(4), 389–392. <https://doi.org/10.3746/pnf.2016.21.4.389>
- Kaur, J., Kandhola, G., Batta-Mpouma, J., Chen, J., Sakon, J., & Kim, J. W. (2021). Enhanced Localized Surface Plasmon Resonance of Gold Nanoparticles Synthesized on Cellulose Nanocrystals. *2021 IEEE 15th International Conference on Nano/Molecular Medicine & Engineering (NANOMED)*, 109–113. <https://doi.org/10.1109/NANOMED54179.2021.9766602>
- Kumar, A., Choudhary, A., Kaur, H., Mehta, S., & Husen, A. (2021). Metal-based nanoparticles, sensors, and their multifaceted application in food packaging. *Journal of Nanobiotechnology*, 19(1), 256. <https://doi.org/10.1186/s12951-021-00996-0>
- Kumari, V., Vishwas, S., Kumar, R., Kakoty, V., Khursheed, R., Babu, M. R., Harish, V., Mittal, N., Singh, P. K., Alharthi, N. S., Hakami, M. A., Aba Alkhayl, F. F., Gupta, G., Rubis, G. D., Pauldel, K. R., Singh, M., Zandi, M., Oliver, B. G., Dua, K., & Singh, S. K. (2023). An overview of biomedical applications for gold nanoparticles against lung cancer. *Journal of Drug Delivery Science and Technology*, 86, 104729. <https://doi.org/https://doi.org/10.1016/j.jddst.2023.104729>
- Kus-Liśkiewicz, M., Fickers, P., & Ben Tahar, I. (2021). Biocompatibility and Cytotoxicity of Gold Nanoparticles: Recent Advances in Methodologies and Regulations. *International Journal of Molecular Sciences*, 22(20), 10952. <https://www.mdpi.com/1422-0067/22/20/10952>
- Lee, E., Jeon, H., Lee, M., Ryu, J., Kang, C., Kim, S., Jung, J., & Kwon, Y. (2019). Molecular origin of AuNPs-induced cytotoxicity and mechanistic study. *Scientific Reports*, 9(1), 2494. <https://doi.org/10.1038/s41598-019-39579-3>
- Lemke, E. A. (2021). Ginseng for the Management of Cancer-Related Fatigue: An Integrative Review. *Journal of the Advanced Practitioner in Oncology*, 12(4), 406–414. <https://doi.org/10.6004/jadpro.2021.12.4.5>
- Liu, H., Lu, X., Hu, Y., & Fan, X. (2020). Chemical constituents of Panax ginseng and Panax notoginseng explain why they differ in therapeutic efficacy. *Pharmacological Research*, 161, 105263. <https://doi.org/https://doi.org/10.1016/j.phrs.2020.105263>
- Milan, J., Niemczyk, K., & Kus-Liśkiewicz, M. (2022). Treasure on the Earth—Gold Nanoparticles and Their Biomedical Applications. *Materials*, 15(9), 3355. <https://www.mdpi.com/1996-1944/15/9/3355>
- Nejati, K., Dadashpour, M., Gharibi, T., Mellatyar, H., & Akbarzadeh, A. (2022). Biomedical Applications of Functionalized Gold Nanoparticles: A Review. *Journal of Cluster Science*, 33(1), 1–16. <https://doi.org/10.1007/s10876-020-01955-9>
- Pourhassan-Moghaddam, M., Zarghami, N., Mohtasenifar, A., Rahmati-Yamchi, M., Gholizadeh, D., Akbarzadeh, A., Guardia, M. d. l., & Nejati-Koshki, K. (2014). Watercress-based gold nanoparticles: biosynthesis, mechanism of formation and study of their biocompatibility in vitro. *Micro & Nano Letters*, 9(5), 345–350. <https://doi.org/doi:10.1049/mnl.2014.0063>
- Rodríguez-León, E., Rodríguez-Vázquez, B. E., Martínez-Higuera, A., Rodríguez-Beas, C., Larios-Rodríguez, E., Navarro, R. E., López-Esparza, R., & Iñiguez-Palomares, R. A. (2019). Synthesis of Gold Nanoparticles Using Mimosa tenuiflora Extract, Assessments of Cytotoxicity, Cellular Uptake, and Catalysis. *Nanoscale Research Letters*, 14(1), 334. <https://doi.org/10.1186/s11671-019-3158-9>
- Semwal, V., Jensen, O. R., Bang, O., & Janting, J. (2023). Investigation of Performance Parameters of Spherical Gold Nanoparticles in Localized Surface Plasmon Resonance Biosensing. *Micromachines*, 14(9), 1717. <https://www.mdpi.com/2072-666X/14/9/1717>
- Shahlaei, M., Azad, A. K., Sulaiman, W. M. A. W., Derakhshani, A., Mofakham, E. B., Mallandrich,

- M., Kumarasamy, V., & Subramaniyan, V. (2024). A review of metallic nanoparticles: present issues and prospects focused on the preparation methods, characterization techniques, and their theranostic applications. *Frontiers in Chemistry*, 12, 1398979. <https://doi.org/10.3389/fchem.2024.1398979>
- Szczuka, D., Nowak, A., Zakłos-Szyda, M., Kochan, E., Szymańska, G., Motyl, I., & Blasiak, J. (2019). American Ginseng (*Panax quinquefolium* L.) as a Source of Bioactive Phytochemicals with Pro-Health Properties. *Nutrients*, 11(5), 1041. <https://www.mdpi.com/2072-6643/11/5/1041>
- Vijayaram, S., Razafindralambo, H., Sun, Y.-Z., Vasantharaj, S., Ghafarifarsani, H., Hoseinifar, S. H., & Raeeszadeh, M. (2024). Applications of Green Synthesized Metal Nanoparticles—a Review. *Biological Trace Element Research*, 202(1), 360–386. <https://doi.org/10.1007/s12011-023-03645-9>
- Wehbe, N., Mesmar, J. E., El Kurdi, R., Al-Sawalmih, A., Badran, A., Patra, D., & Baydoun, E. (2025). Halodule uninervis extract facilitates the green synthesis of gold nanoparticles with anticancer activity. *Scientific Reports*, 15(1), 4286. <https://doi.org/10.1038/s41598-024-81875-0>
- Werner, S. J., Shwiff, S. A., Elser, J. L., Kirkpatrick, K. N., Pettit, S. E., Suckow, J., Willging, R. C., Tharman, J. A., & Heil, J. (2014). Perceived impacts of wild turkeys and management techniques for Wisconsin ginseng production. *Crop Protection*, 65, 221–226. <https://doi.org/https://doi.org/10.1016/j.cropro.2014.08.004>
- Zhang, Y.-J., Gan, R.-Y., Li, S., Zhou, Y., Li, A.-N., Xu, D.-P., & Li, H.-B. (2015). Antioxidant Phytochemicals for the Prevention and Treatment of Chronic Diseases. *Molecules*, 20(12), 21138–21156. <https://www.mdpi.com/1420-3049/20/12/19753>



Publisher's note: Eurasia Academic Publishing Group (EAPG) remains neutral with regard to jurisdictional claims in published maps and institutional affiliations.

Open Access. This article is licensed under a Creative Commons Attribution-NoDerivatives 4.0 International (CC BY-ND 4.0) licence, which permits copy and redistribute the material in any medium or format for any purpose, even commercially. The licensor cannot revoke these freedoms as long as you follow the licence terms. Under the following terms you must give appropriate credit, provide a link to the license, and indicate if changes were made. You may do so in any reasonable manner, but not in any way that suggests the licensor endorsed you or your use. If you remix, transform, or build upon the material, you may not distribute the modified material. To view a copy of this license, visit <https://creativecommons.org/licenses/by-nd/4.0/>.